Estimation of baseflow recession constants and effective hydraulic parameters in the karst basins of southwest China

Xi Chen, Yan-fang Zhang, Xianwu Xue, Zhicai Zhang and Lingna Wei

ABSTRACT

By analysing the hydrographs of karst basin outflow, it is possible to identify aquifer characteristics and, accordingly, the main features of a karst basin. In this study, 19 basins with daily observed flow discharges during drought periods between October and April 1973–1983 were selected to analyse the master recession curve (MRC). During a drought period, the MRCs were separated into segments of fast flow exponential recession and slow flow exponential recession. Break points of the fast and slow recession segments were identified and the recession constants α were determined. Relationships between α and basin area were identified. According to the estimated baseflow recession constants, hydraulic parameters including aquifer thickness and hydraulic conductivity were estimated. Hydraulic conductivities in the near-surface epikarst aquifer are of the order 10^{-3} m s^{-1}, much larger than 10^{-5} m s^{-1} in the low-permeability aquifer.

Key words | baseflow recession constant, hydraulic conductivity, karst, master recession curve, recession analysis

Xi Chen (corresponding author)
Yan-fang Zhang
Xianwu Xue
Zhicai Zhang
Lingna Wei
State Key Laboratory of Hydrology-Water Resources and Hydraulic Engineering,
Hohai University,
Nanjing 210098,
China
E-mail: *xichen@hhu.edu.cn*

INTRODUCTION

Karst terrain covers about 15% of the world's land area or about 2.2 million km^2, and is home for around 1 billion people (17% of the world's population) (Yuan & Cai 1988). About 25% of the world's population is supplied largely or entirely by karst waters, including deep carbonate aquifers (Ford & Williams 1989). One of the largest continuous karst areas in the world is located in the Yunnan–Guizhou Plateau of southwest China. It covers 540,000 km^2 and has a population of 100 million. In the karst region of southwest China, soils developed on carbonate rocks are generally 30–50 cm thick. In Guizhou province located in the centre of the southwest karst region, about 73% of the land surface is karst which is underlain by up to 10,000 m of soluble carbonate rocks. Ninety-seven percent is hilly and only 3% is classified as flat (Zeng 1994). Mountainous areas with slopes of more than 15° account for 60% of its area (Li *et al.* 2002). The region contains a full suite of karst landforms including poljes, cockpits, towers and dolines.

Karstic watershed outflow depends strongly on rock dissolution and geomorphology. Because of the effects of CO_2 supply and water flow on soluble carbonate rocks, the network of epikarst fissures through which percolation water passes is widened by dissolution near the surface. Epikarst near the surface therefore has a large permeability, offering a fast water infiltration. As the extent and frequency of widening diminishes gradually with depth, epikarst permeability diminishes with depth (Ford & Williams 2007). Limestone fracture aperture may be as large as 1×10^{-2} m in the exposed surface, decreasing to 1×10^{-3} to 1×10^{-4} m in compact and impermeable bedrock (Singhal & Gupta 1999). Consequently, after recharge percolating rainwater is retained near the base of the epikarst leading to the formation of an epikarstic aquifer (Williams 2008). Part of the temporarily stored water flows out as a spring, and the remainder flows via the vertical shaft system into conduit systems of the deep aquifer. Groundwater in the deep

doi: 10.2166/nh.2011.136

aquifer flows through interconnected, solutionally enlarged conduits and cave systems and eventually flows out of the basin as a spring.

Baseflow therefore comes from a shallow epikarst aquifer and a deep aquifer. Epikarst aquifer at 10 cm to 30 m depth offers fast flow (Klimchouk 2000). The perched water could be retained in the epikarst zone for some days to several months (Gunn 1983; Williams 1983; Klimchouk 1997). Characteristics of the deep aquifer are strongly affected by karstic morphology (Wang 1999). According to investigations of Wang (1999) and Yang (1982) along the large rivers in the karst areas of Guizhou province of China, the deep aquifer thickness increases from the upstream areas to the downstream areas. In the upstream plateau areas where the rivers originate, the water table is less than 50 m below the ground surface. In the downstream gorge areas, the deep aquifer closely connects with the deep incised valleys of 300–700 m in depths. Groundwater flow converges towards underground channels and eventually drains into the deep incised rivers. The water table could be as large as 100 m below the surface in the downstream areas.

The baseflow recession curve allows quantitative comparisons between karst aquifers. Theoretically, factors that determine the baseflow hydrograph include area of groundwater basin, degree of conduit development and hydraulic gradient from input to output. When quantifying hydraulic properties from baseflow hydrographs, the interpretation is that water flowing through portions of the karst aquifer with different conductivities produces the distinctive shape of the baseflow recession hydrograph.

An exponential recession equation is commonly used for describing baseflow recession (Milanovic 1981; Padilla *et al.* 1994; Shevenell 1996; Baedke & Krothe 2001). This method is based upon a Darcian theory of flow, which is applicable to many karst catchments where the storage of the conduit system is much smaller than that of the fissured matrix blocks (Atkinson 1977; Sauter 1992; Kovács *et al.* 2005; Birk & Hergarten 2010). Baedke & Krothe (2001) and Kovács *et al.* (2005) found that the exponential recession may not be valid for higher flow rates through the conduit. Kovács *et al.* (2005) suggested a threshold value for dividing the recession curve into two stages: an early, non-exponential stage of flow recession and a long-term, exponential stage of flow recession. Early recession behaviour strongly depends on the initial conditions of individual storms and can change through time due to variability in factors such as the areal distribution of rainfall, residual storage in connected surface water bodies, catchment wetness, saturated aquifer thickness or depth of stream penetration into the aquifer (Birk & Hergarten 2010).

Kovács *et al.* (2005) also noticed that by exceeding the threshold value the conduit had no further influence on the baseflow recession, and that the recession process is controlled by the hydraulic parameters of the low-permeability blocks alone. Trček (2007) pointed out that in the case of a small storage volume of aquifer, most of the water is retained and stored in the base of the epikarst zone and this water slowly seeps through tiny fractured rock blocks and diffusely recharges aquifer lower parts. Baseflow during a non-rainfall period of the drought season could therefore be regarded as groundwater mostly from tiny fractured rock blocks which follows exponential recessions. If a master recession curve (MRC) was created using a series of recession curves during the drought period, the fast and slow recession segments of an MRC during a drought period reflects the hydraulic behaviour of the high- and low-permeability fractures, which can be determined by the recession coefficients or constants from the straight-line segments of natural logarithm of Q (discharge) versus t (time), or ln Q vs t.

In this study, baseflow recession curves were analysed according to daily observation data of flow discharges during recession periods in 19 basins of Wujiang watershed, southwest China. An MRC was created for each basin during the drought period and separated into two segments through ln Q vs t analysis. The recession constants of two baseflow recession segments and their relationship with basin areas were determined. The recession constants were further used for estimation of effective hydraulic parameters of the karst basins which have not been reported previously.

METHODOLOGY

The total recession curve can be represented as the sum of two, three or more exponential functions for groundwater flow in the porous or fractured medium:

$$Q(t) = \sum_{i=1}^{N} Q_{0i} e^{-\alpha_i t} \quad (1)$$

where N is the number of exponentials, t is the time, Q_{0i} are the discharges at $t = 0$ and α_i are the recession constants for each exponential recession. In well-developed karst systems, three straight-line segments of ln Q vs t with different values of α_i occur in the recession. The first and steepest slope represents the dominant effects of drainage of the larger karst features of the conduit. The second slope is dominated by the intermediate storage features (fractures). The third slope represents drainage of the matrix portion of the aquifer (Shevenell 1996).

The short and fast recession of the first segment mostly occurs for the heavy storms during the rainfall season when the groundwater table is high and karst systems are strongly influenced by concentrated allogenic recharge and significant storage in conduits, open channels or reservoirs. For the master recession curve during the drought periods, if the fast recession of the storm water from conduits can be neglected, two straight-line segments are able to approximate the MRC. The two recession segments represent the rapid and slow depletions of flows from the high-permeability fractures and the low-permeability fracture network, respectively.

The recession constants are determined from the slope of the recession curve when the recession hydrograph is plotted on a semi-logarithmic graph. Recession constants depend on geomorphologic conditions and watershed features and present spatial and temporal differences, particularly for individual flow recession analysis. The estimated recession constant was 0.027 day^{-1} for the recession stage after approximately 20 days in the catchment area of Cheddar spring, Mendip Hill, Great Britain (Atkinson 1977). Sauter (1992) identified a distinct exponential behaviour with a recession coefficient of 0.017 day^{-1} over a wide range of discharge for the Gallusquelle catchment situated on the karst plateau Swabian Alb in southwest Germany. Kovács *et al.* (2005) graphically represented the baseflow recession coefficient associated with aquifer hydraulic and geometric parameters in the Milandrine headwater catchment of NW Switzerland. For example, the recession coefficient is 0.0028 day^{-1} for the parameters of storability of 0.001, frequency of conduits of 0.005 day^{-1} and transmissivity of the low-permeability matrix of 6.5×10^{-7} m^2 s^{-1}. Investigations by Guo (2007) revealed that, for the two recession segments in the fractured medium of Houzhai catchment nearby Sanchahe (SCH) of the study watershed, the recession constant is within 0.0129–0.032 day^{-1} for the rapid depletion of flow from the high-permeability karst fractures and within 0.00262–0.0035 day^{-1} for the low depletion of flow from the low-permeability fractures.

Rorabaugh (1964) proposed the following equation to calculate properties of the aquifer using the recession constants:

$$T = \alpha 4 S_y L^2 / \pi^2 \tag{2}$$

where α is the slope of the discharge hydrograph, T is transmissivity, S_y is specific yield and L is distance from the discharge point to the drainage divide. If the recession process is controlled by the hydraulic parameters of the low-permeability blocks alone, Equation (2) provides an adequate characterization of the system's overall response (Kovács *et al.* 2005).

Equation (2) is rearranged to estimate the hydraulic parameters of an unconfined aquifer from baseflow recession curves (Atkinson 1977):

$$\log\left(\frac{Q_1}{Q_2}\right) = \frac{T}{S_y}(t_2 - t_1)\frac{1.071}{L^2} \tag{3}$$

Equation (3) is further rearranged so that the ratio of transmissivity to specific yield (T/S_y) for each segment of the recession curve can be calculated once a value of L is estimated and the slope of each segment of the recession curve is known, i.e.

$$\frac{T}{S_y} = \frac{\log(Q_1/Q_2)}{(t_2 - t_1)}\frac{L}{1.071} \tag{4}$$

STUDY AREA AND SITE DESCRIPTION

The Wujiang River drains from the Yunnan–Guizhou Plateau, and is the largest tributary of the Yangtze River (Figure 1). The mainstream length of the Wujiang River is 874 km, with an area of 66,849 km^2 and a mean water discharge of 1,295 m^3 s^{-1}. The region has a complex topography ranging in elevation from 300 to 2,900 m, and a sub-tropical and humid monsoonal climate with a mean

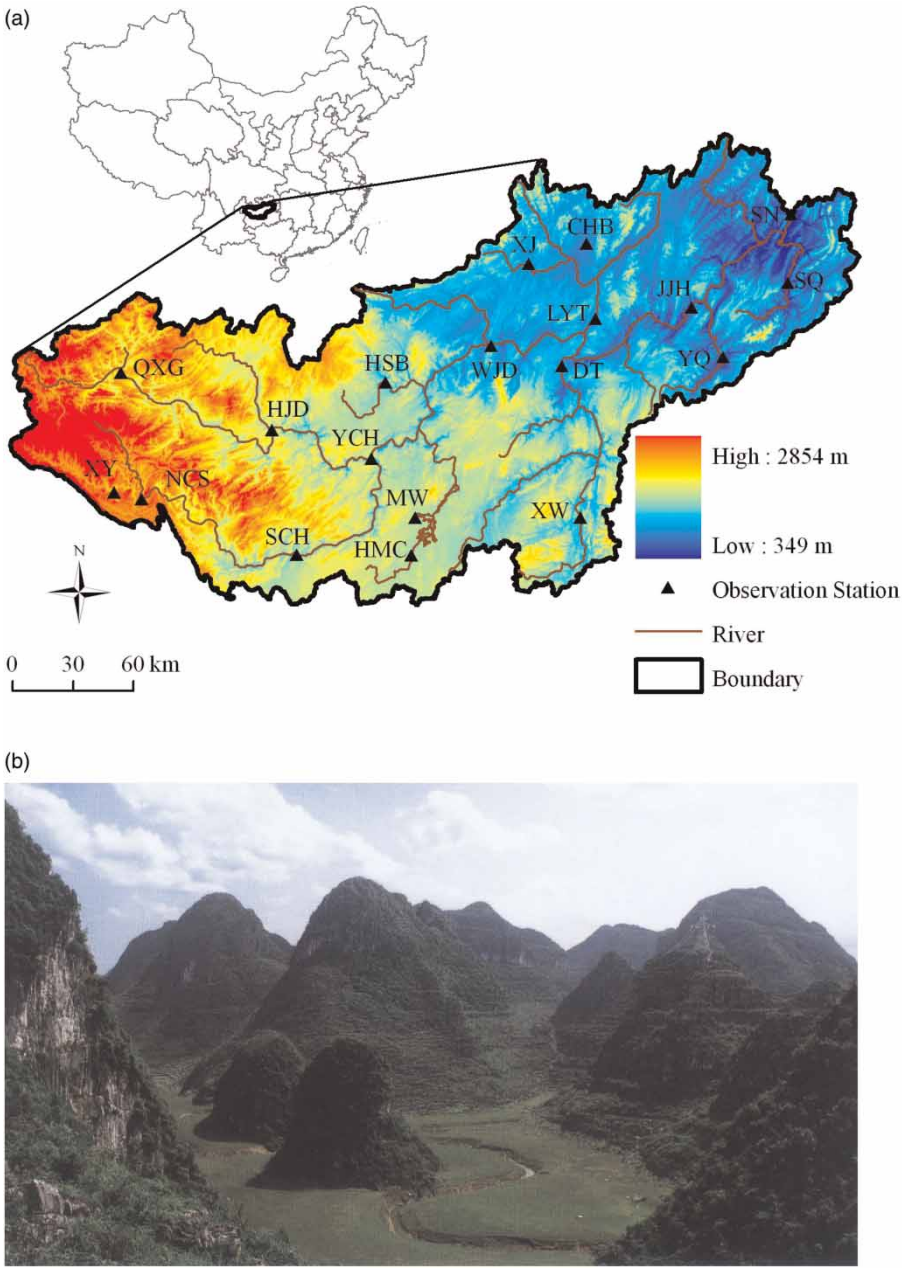

Figure 1 | (a) Basin topography and location of observation stations and (b) photo of landscape.

annual temperature of 9–17 °C and mean annual precipitation of 900–1,400 mm. Annual precipitation decreases from south to north and from east to west. The precipitation in summer during June–September accounts for about 50% of the annual precipitation.

The strata exposed in the Wujiang River watershed are mainly Pre-Jurassic in age (Figure 2). Geology in the upper reaches of the Wujiang River watershed is dominated by Permian and Triassic carbonate rocks. In the middle reaches are widely distributed Permian and Triassic limestones, dolomitic limestones and dolomites, while in the lower reaches are mainly carbonate rocks as well as shales, sand shales and siltstones (Han & Liu 2004). Carbonate rock occupies about 70% of the total area. The upper reach

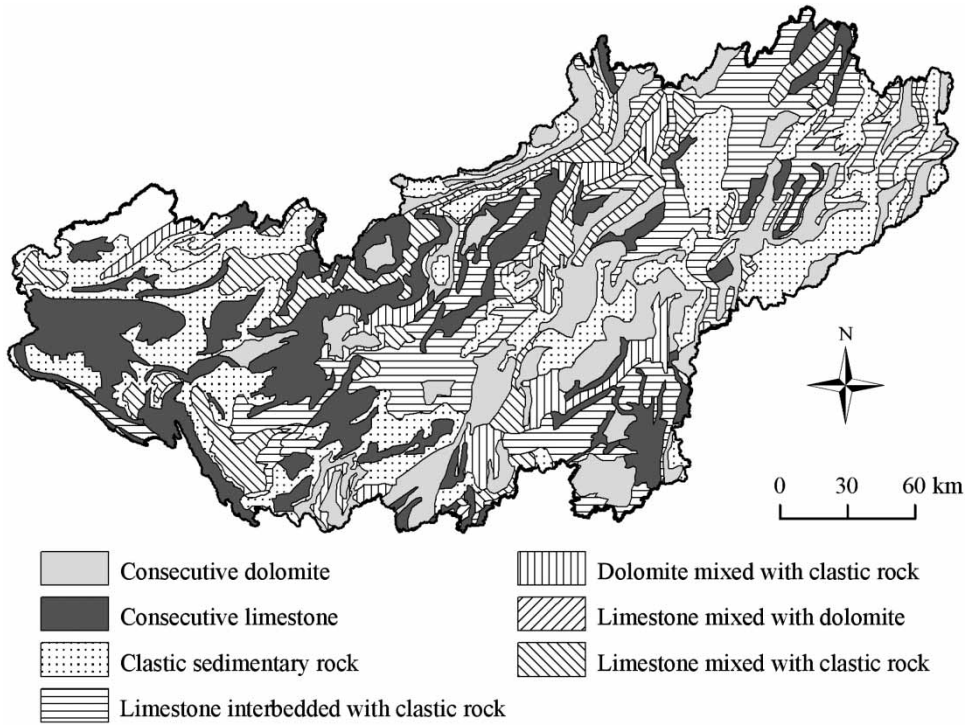

Figure 2 | Basin geology.

areas are covered with calcareous soils and shrubs, while the remaining areas are calcareous and yellow soils and arbor-shrub vegetation.

Since the Mid-Pleistocene, crustal movement has been dominated by intermittent uplifting over a vast area, accompanied by local uplifting. The alternation of upliftings and stages of relative rest have occurred more frequently and intensively towards the present day. Uplifting and strong water erosion of solutional carbonate rock by stream flow resulted in the deep incised valleys and rugged relief of landscape. Study results by Li (2001) demonstrate that the valley depth along the mainstream of Wujiang River reaches 300–500 m below the ground surface in the east and middle of the watershed and 500–700 m in the west. Depth to groundwater table is related to the karst geomorphologic features. Investigations by Yang (1982) indicated that shallower groundwater tables occur in the upstream areas where topography varies between 1,100 and 1,250 m in elevation and surface slopes are gentle (e.g. Sanchahe (SCH) River in Figure 3). Depth to groundwater table varies from less than 10 m in the karst troughs and gullies to 30 m near rivers. Groundwater depth between 50 and 100 m is located between the terrace fringe and the upstream areas of the highland first table (e.g. in the areas of Hongjiadu (HJD), Qixingguan (QXG), Yachihe (YCH) and Xiangyang (XY) in Figure 1). Groundwater depths of greater than 100 m can be found in the deep incised valleys of middle and downstream areas of the Wujiang River. The depth to groundwater table and its connection with river valleys indicate features of fractured aquifer systems and determine baseflow recession behaviour.

For investigation of baseflow recession constants and hydraulic parameters, 19 basins in the upper stream of Sinan station with daily streamflow observation data from 1973 to 1983 (Figure 1) were selected. The eight basins – Qixingguan (QXG), Xiangyang (XY), Changheba (CHB), Xiangjiang (XJ), Huoshiba (HSB), Xiawan (XW), Yuqing (YQ) and Shiqian (SQ) – are located in the uppermost tributaries. Four hydrological stations of Yachihe (YCH), Wujiangdu (WJD), Jiangjiehe (JJH) and Sinan (SN) are located in the main stream. The selected basin areas vary from the smallest of 203 km^2 for Maiweng (MW) basin to the largest of 50,791 km^2 for Sinan (SN) basin.

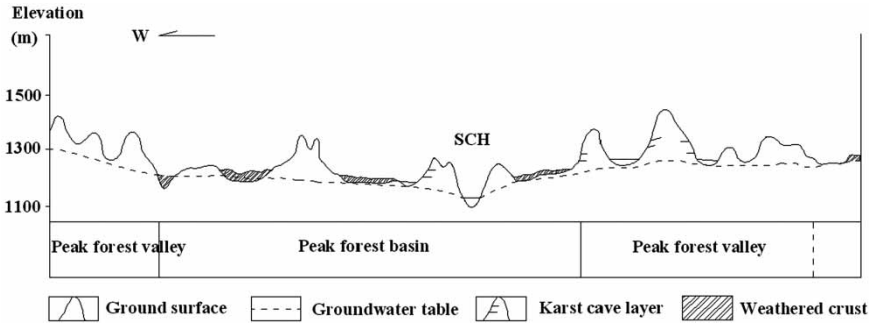

Figure 3 | Cross-section of geomorphology and groundwater table nearby SCH (Yang 1982).

RESULTS

Analysis of baseflow recession curve

To reduce the variability of the recession behaviour affected by rainfall, catchment wetness and saturated aquifer thickness, hydrographs in the drought period were selected for creating the MRC. Long-term data of discharges for the period 1973–1983 were used in this analysis. According to monthly variations of precipitation in the study area, the period from October to April is relatively dry (Yang *et al.* 2009). Extracted curves comprise recession curves for the months October–April for the following year. Several individual segments of continuous recession were selected, during which each pair of consecutive daily values must meet the condition that the first value exceeds or is equal to the second. The MRC was built based on the lowest 'tails' of the recessions and curves are sorted in decreasing order by use of MRC tool (see Figure 4 as an example).

In hydrological practice it is customary to represent the recession curves graphically with a semi-logarithmic plot, so that discharge Q is plotted on the logarithmic ordinate and time t is plotted on the normal abscissa. The relationship of Equation (1) will then appear as a straight line. Following Kovács *et al.* (2005), it was assumed that the point of inflection on the falling limb of the hydrograph marks the end of the early recession and thus the start of the long-term recession.

Figure 5 shows that the MRC can be fitted well by two segments of ln Q vs t lines. Only a few initial discharges in the early MRC (Figure 5) were underestimated. The correlation between the MRC and fitted curve for the early and long-term recession segments was very high, showing the good quality of fit (Figure 5). For 19 basins, the correlation coefficients (CE) between MRC and fitted curve are larger than 0.921 (Table 1). By fitting the function expressed in Equation (1) to the MRCs, the coefficient of α_i was calculated according to the slope of the ln Q vs t line (Figure 5). For 19 basins, the MRC can be separated into two segments. The recession constant on average in Table 1 is 0.082 day^{-1} for the first recession period, much larger than 0.0094 day^{-1} for the second recession period. This finding indicates that the fast flow during the first recession

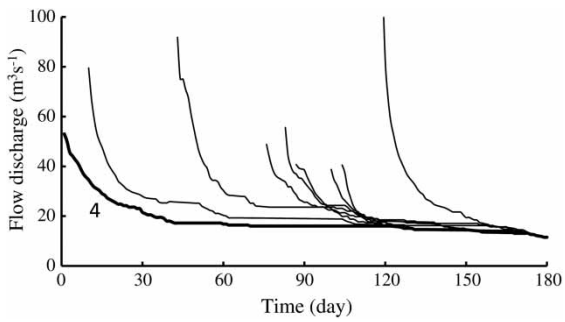

Figure 4 | Recession curve in the Qixingguan (QXG) basin.

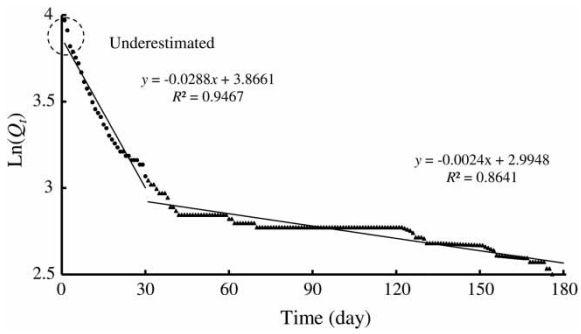

Figure 5 | ln Q_t versus t for Qixingguan (QXG) basin.

period comes from the high-permeability aquifer and the slow flow during the second recession period from the low-permeability aquifer. The fast recession period lasts around 30 days for most basins with areas larger than 2,000 km^2, and lasts for a shorter time as the basin area decreases. For the small basins of CHB, XJ, MW and HMC, the fast recession period lasts less than 10 days (Table 1).

Baseflow recession constants related to basin area

Among the 19 basins, 11 sub-basins were selected from the tributaries of the Wujiang River. Basin areas vary from 203 km^2 for the smallest MH basin to 2,970 km^2 for the largest QXG basin (Figure 1). Baseflow recession constants for the two segments (α_1 and α_2 in Figure 6) were found to be strongly related to basin areas (Figure 6). A power law function fits the relationship of the recession constants with basin areas well. For basin areas less than 1,000 km^2, the recession constants decrease rapidly as area increases. As basin area increases from 1,000 to 3,000 km^2, the recession constants decrease slowly. For the extremely large basins of over 3,000 km^2, such as Yachihe (YCH), Wujiangdu (WJD), Jiangjiehe (JJH) and Sinan (SN) in the mainstream of the Wujiang River, the recession constants are less correlated with basin areas. The recession constants averaged for the four large basins are 0.036 and 0.006 day^{-1} for the first and second segments, respectively (α_1 and α_2 in Table 1).

Hydraulic parameters derived from baseflow recession constants

According to Equations (3) and (4) hydraulic parameters of T/S_y for the two segments can be calculated once the recession constants are estimated, i.e.

$$\alpha = \frac{\log(Q_1/Q_2)}{t_2 - t_1}$$

Table 1 | Basin characteristics of recession curves

No.	Station name	Basin area (km^2)	Fast recession segment Initial discharge Q_{01} (m^3 s^{-1})	α_1 (day^{-1})	Slow recession segment Initial discharge Q_{02} (m^3 s^{-1})	α_2 (day^{-1})	Period of fast segment (days)	Correlation coefficient
1	Qixingguan (QXG)	2,970	47.754	0.029	19.980	0.002	30	0.979
2	Xiangyang (XY)	850	38.276	0.074	8.442	0.010	19	0.984
3	Niuchishui (NCS)	2,210	63.873	0.044	19.735	0.007	33	0.988
4	Hongjiadu (HJD)	7,492	197.04	0.036	75.251	0.004	27	0.987
5	Sanchahe (SCH)	5,452	80.525	0.056	31.261	0.008	19	0.991
6	Yachihe (YCH)	16,541	352.72	0.027	107.60	0.005	50	0.994
7	Huoshiba (HSB)	1,527	22.363	0.038	9.629	0.006	22	0.952
8	Wujiangdu (WJD)	26,496	642.05	0.033	244.31	0.009	30	0.989
9	Changheba (CHB)	505	54.286	0.287	7.105	0.020	6	0.983
10	Xiangjiang (XJ)	553	6.862	0.155	3.611	0.013	4	0.967
11	Liyutang (LYT)	4,735	184.94	0.075	27.003	0.009	30	0.952
12	Xiawan (XW)	1,485	15.460	0.041	6.695	0.007	22	0.981
13	Dongtou (DT)	6,917	219.43	0.064	58.154	0.008	25	0.950
14	Jiangjiehe (JJH)	43,292	1,069.7	0.046	342.10	0.006	25	0.981
15	Yuqing (YQ)	764	28.304	0.074	3.784	0.008	30	0.973
16	Shiqian (SQ)	1,112	6.024	0.022	3.684	0.006	37	0.983
17	Sinan (SN)	50,791	1,183.1	0.039	537.15	0.009	31	0.980
18	Maiweng (MW)	203	12.445	0.141	4.674	0.019	7	0.955
19	Huangmaocun (HMC)	741	64.192	0.269	7.902	0.021	6	0.921

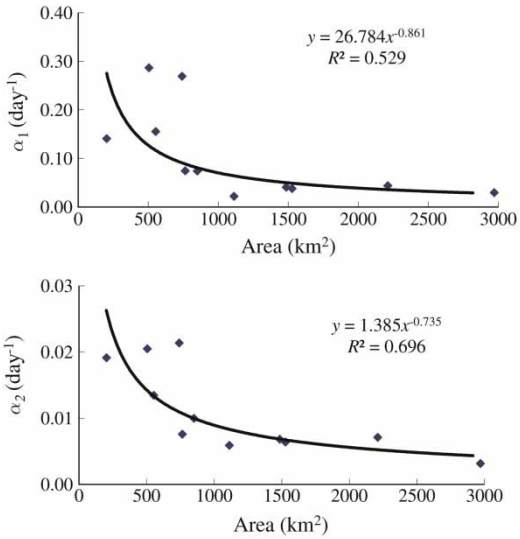

Figure 6 | Relationship between the recession constants and basin areas.

in Equation (4), and the basin characteristic of the distance from the river to the drainage divide L is known.

Although detailed information of the variable L can be obtained by tracing experiments (Baedke & Krothe 2001), it is not available for most karst basins. It is common practice to assign each discharge location a value of L that is measured from the river to the topographically defined groundwater drainage divide (Teutsch 1992; Shevenell 1996). Although the boundaries of the drainage divide can change spatially and temporally under different aquifer conditions for individual storm flows in the karst basin, the MRC during the drought reflects the overall storage characteristics of the watershed (Lamb & Beven 1997). An average value of L was therefore calculated for the drought period, representing the mean of the distances to the topographically defined drainage boundary in both sides of the discharge point (L_1 and L_2 in Figure 7). Table 2 shows that L varies from 4.03 km for the smallest basin of MW to 19.72 km for the NCS basin.

The calculated values of T/S_y for the fast and slow segments are listed in Table 2. These values of T/S_y can be used to further estimate hydraulic conductivities if specific yield S_y and thickness of the karst aquifer are known. Field investigations of a profile of SCH catchments demonstrate that karst fracture porosity is dramatically reduced from 6.9% for the epikarst layer (less than 2 m) to 1.0% at a depth of 5 m (Figure 8). As the MRC in the drought period could be regarded as water from the base of the epikarst aquifer, the fracture porosity of epikarst could be regarded as 1.0% for the SCH catchment. Numerous analyses carried out in many other regions of the world (Bonacci 1987) showed that the effective porosity ($\leq$ fracture porosity) amounts to 0.1–1% on average and the extent and frequency of fracture widening diminishes with depth (Ford & Williams 2007). Thus, 1% was selected as an approximate S_y value for the high-permeability fractures (in which the baseflow comes from water storage in the epikarst zone during the fast recession period) and 0.1% as the S_y value for the low-permeability fractures (in which the baseflow comes from the deep fractured rock blocks during the slow recession period).

Fast flow recession of MRC starts from an initial flow discharge Q_{01} from the high-permeability fractures of the epikarst aquifer. Because storm flow can be neglected in the drought period, this fast flow aquifer could be regarded as just below valley bottoms where a relatively steady-state flow from the fractured media accounts for the exponential recession behaviour. The aquifer thickness at time t_1 (H_{t1}) corresponding to initial flow discharge Q_{01} in Table 1 is determined by measuring the distance between connection lines of valley bottoms in the cross-section and the mainstream bottom (Figure 6). The estimated aquifer thickness ranges from 17.40 m for the upstream of HMC tributary to 183.46 m for YCH in the mainstream of the Wujiang River (Table 2).

It can be seen that estimated aquifer thickness reflects water flow and geomorphic effects on groundwater storage. Because of strong rock dissolution due to groundwater flow concentration towards the downstream, the aquifer becomes thicker in the downstream areas. For example, the aquifer

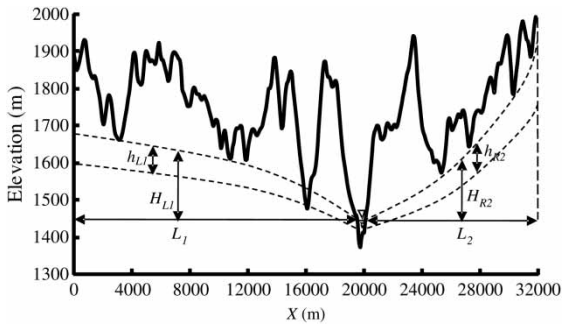

Figure 7 | Schematic of cross-section indicating aquifer thickness (H_{L1} and H_{L2}), decline of groundwater table (h_{L1} and h_{L2}) and distance from the discharge point to the drainage divide (L_1 and L_2).

Table 2 | Estimated basin aquifer features and hydraulic parameters

No.	Station name	L (km)	H_{t1} (m)	h_1 (m)	T/S_{y1} ($m^2\ s^{-1}$)	T/S_{y2} ($m^2\ s^{-1}$)	K_1 (10^{-3} m s^{-1})	K_2 (10^{-5} m s^{-1})
1	Qixingguan (QXG)	17.27	132.72	2.870	41.141	4.416	0.775	0.832
2	Xiangyang (XY)	9.81	87.62	3.970	33.363	4.503	0.952	1.285
3	Niuchishui (NCS)	19.72	107.78	4.362	79.769	12.974	1.850	3.009
4	Hongjiadu (HJD)	13.18	143.40	3.912	29.558	3.353	0.515	0.585
5	Sanchahe (SCH)	15.47	161.97	1.494	62.750	8.451	0.969	1.304
6	Yachihe (YCH)	13.49	183.46	5.060	23.020	3.930	0.314	0.536
7	Huoshiba (HSB)	16.64	89.64	1.890	49.075	8.313	1.369	2.318
8	Wujiangdu (WJD)	12.86	164.64	4.001	25.360	7.025	0.385	1.067
9	Changheba (CHB)	5.91	61.54	2.660	46.974	3.359	1.909	1.365
10	Xiangjiang (XJ)	9.13	48.40	0.319	60.733	5.263	3.137	2.718
11	Liyutang (LYT)	9.95	81.60	4.035	34.694	4.173	1.063	1.279
12	Xiawan (XW)	11.18	53.47	1.309	23.797	4.003	1.113	1.871
13	Dongtou (DT)	10.33	136.83	3.427	31.906	3.871	0.583	0.707
14	Jiangjiehe (JJH)	11.87	149.98	3.166	30.523	3.902	0.509	0.650
15	Yuqing (YQ)	7.55	57.73	3.840	19.888	2.028	0.861	0.878
16	Shiqian (SQ)	13.06	130.61	1.186	17.533	4.720	0.336	0.903
17	Sinan (SN)	11.73	96.10	3.616	25.249	5.883	0.657	1.530
18	Maiweng (MW)	4.03	17.50	2.359	10.722	1.458	1.532	2.082
19	Huangmaocun (HMC)	6.16	17.40	2.228	47.832	3.798	6.871	5.456

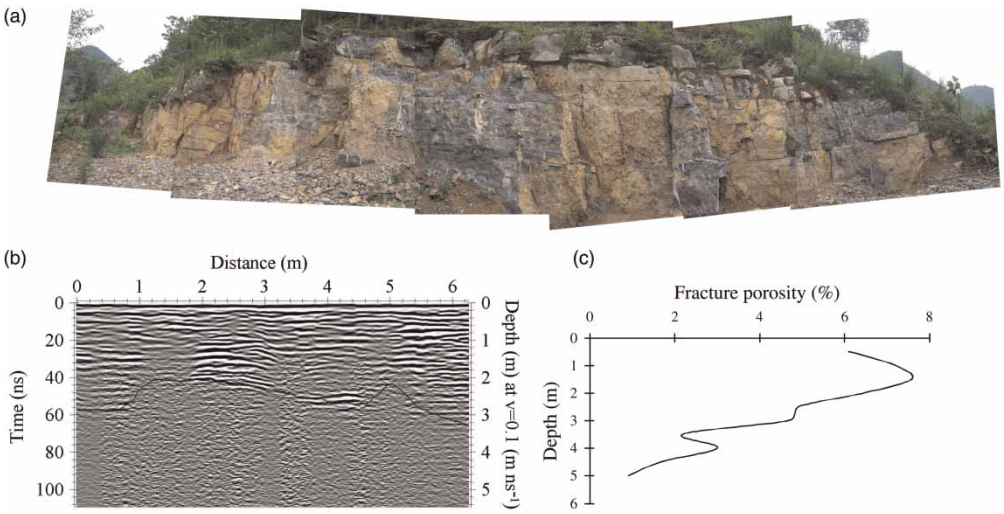

Figure 8 | (a) Photo of a hill profile in SCH, (b) ground-penetrating radar profile and (c) vertical variation of fracture porosity.

thickness near both sides of the SCH River is 87.62 m at the upstream station of XY, and increases to 107.78 and 161.97 m at the middle and downstream stations of NCS and SCH, respectively (Table 2). The relatively smaller aquifer thicknesses of less than 20 m for MW and HMC are located in the broad and shallow river valleys of the upper tributary with a gentle hydraulic gradient of 0.16–0.3% (Figure 3). The estimated aquifer thickness is 17.50 m for MW and 17.40 m for HMC, which are in agreement with field investigation results of less than 20 m by Yang (1982). The larger

aquifer thicknesses over 100 m for HJD, YCH, WJD and JJH are located in both sides of the deep incised mainstream of the Wujiang River.

As shown in Figure 7, the decline of the groundwater table from the high-permeability fractures of the epikarst aquifer during the fast recession period is h_{L1} and h_{R1}, the decline in the left and right sides of the valley, respectively. The decline can be estimated as:

$$S_y h_1 = 10^{-6} Q_{01} \int_0^{T_1} e^{-\alpha_1 t}\, dt/A \quad (5)$$

or

$$h_1 = 10^{-6} Q_{01}(1 - e^{-\alpha_1 T_1})/(\alpha_1 S_y A) \quad (6)$$

where h_1 is the estimated mean value of the groundwater table decline in the left and right sides of the valley, Q_{01} is initial discharge of the fast recession segment, T_1 is period of the fast recession segment and A is basin area. The aquifer thickness of the low-permeability fractures in the slow recession period H_{t2} is therefore

$$H_{t2} = H_{t1} - h_1 \quad (7)$$

The estimated mean value of the groundwater table reduction h_1 for the 19 basins is 2.93 m, varying from 0.32 m for XJ basin to 5.06 m for YCH basin during the fast recession periods of 4 days and 50 days, respectively. h_1 can be regarded as the decline of groundwater in the high-permeability fractures of epikarst zone, which is about 2 m on average for Guizhou province of China according to field investigations by Jiang (1998) and 3–4 m in SCH according to investigations by ground-penetrating radar (Figure 8). The decline of the groundwater table during the fast recession period is much smaller than initial aquifer thickness.

The estimated hydraulic conductivity of the fast recession period K_1 is, on average, 1.35×10^{-3} m s^{-1}, varying from 0.314×10^{-3} m s^{-1} for the YCH basin to 6.871×10^{-3} m s^{-1} for the HMC basin. The estimated hydraulic conductivity of the slow recession period K_2 is, on average, 1.60×10^{-5} m s^{-1}, varying from 0.53×10^{-5} m s^{-1} for the YCH basin to 5.46×10^{-5} m s^{-1} for the HMC basin. The estimated hydraulic conductivity in Table 2 is within the ranges between 10^{-6} and 10^{-2} m s^{-1} for karst limestone (Chiasson *et al.* 2000).

CONCLUSIONS

Characteristics of baseflow recession are very important for investigation of strategies of water resources utilization and ecologic protection in the karst region of southwest China. Aquifer hydraulic parameters are essential for groundwater modelling and water resources estimation in the karst region. In this study, 19 basins in the Wujiang watershed were selected for investigation of baseflow recession characteristics and determination of hydraulic parameters.

The following results were obtained from this study:

1. Although the early stage of individual storm flow recession may deviate from exponential behaviour and the recession constant can change through time due to effects of large fractures and conduits, the MRC during the drought period can be simulated using exponential functions for describing groundwater flow in the fractured media. The fast and slow recessions of the MRC could represent flow recessions from the higher permeability fractures and the lower permeability aquifer, respectively.
2. The recession constants for the two periods decrease significantly with increasing basin area for the relatively small basins with areas less than 1,000 km^2. As the basin areas increase to 3,000 km^2, the basin areas have less influence on the recession constants.
3. Hydraulic conductivity of the high-permeability fractures of epikarst aquifer is estimated to be of the order 10^{-3} m s^{-1} according to the fast recession. This value is much larger than 10^{-5} m s^{-1} for the low-permeability aquifer during the slow recession period. The shallow aquifers in the upstream areas usually have large hydraulic conductivities, e.g. 6.871×10^{-3} m s^{-1} and 5.456×10^{-5} m s^{-1} for the high- and low-permeability fractures in HMC, respectively. Comparatively, the deep aquifers located in the deep incised mainstream have small hydraulic conductivities, e.g. 0.314×10^{-3} m s^{-1} and 0.536×10^{-5} m s^{-1} for the high- and low-permeability fractures in SCH, respectively.

ACKNOWLEDGEMENTS

This research was supported by the National Natural Scientific Foundation of China (No. 40930635, 51079038),

the Programme of Introducing Talents of Discipline to Universities (No. B08048) and the Program for Changjiang Scholars and Innovative Research Team in University, China. We are grateful to the editor and two anonymous reviewers for their constructive comments on the earlier manuscript, which resulted in an improvement of the paper.

REFERENCES

Atkinson, T. C. 1977 Diffuse flow and conduit flow in limestone terrain in the Mendip Hills, Somerset (Great Britain). *J. Hydrol.* **35** (1–2), 93–110.

Baedke, S. J. & Krothe, N. C. 2001 Derivation of effective hydraulic parameters of a karst aquifer from discharge hydrograph analysis. *Water Resour. Res.* **37** (1), 13–19.

Bonacci, O. 1987 *Karst Hydrology*. Springer Verlag, Herdelberg, Germany.

Birk, S. & Hergarten, S. 2010 Early recession behaviour of spring hydrographs. *J. Hydrol.* **387** (1–2), 24–32.

Chiasson, A., Rees, S. J. & Spitler, J. D. 2000 A preliminary assessment of the effects of ground-water flow on closed-loop ground-source systems. *ASHRAE Transactions* **106** (1), 380–393.

Ford, D. C. & Williams, P. W. 1989 *Karst Geomorphology and Hydrology*. Unwin Hyman, London.

Ford, D. C. & Williams, P. 2007 *Karst Hydrogeology and Geomorphology*. Wiley, Chichester, 576 pp.

Gunn, J. 1983 Point recharge of limestone aquifers – a model from New Zealand karst. *J. Hydrol.* **61**, 19–29.

Guo, C. 2007 *China Karst Ecohydrology*. Geological Publishing House, Beijing, China.

Han, G. L. & Liu, C. Q. 2004 Water geochemistry controlled by carbonate dissolution: a study of the river waters draining karst-dominated terrain, Guizhou Province, China. *Chem. Geol.* **204** (1–2), 1–21.

Jiang, Z. C. 1998 Features of epikarst zone in south China and formation mechanism. *Tropical Geography* **18** (4), 322–326.

Klimchouk, A. B. 1997 The nature and principal characteristics of epikarst. In *Proceedings of 12th International Congress of Speleology*, La Chaux-de-Fonds, 306 pp. La Chaux-de-Fonds, Switzerland.

Klimchouk, A. B. 2000 The formation of epikarst and its role in vadose speleogenesis. In: *Speleogenesis. Evolution of Karst Aquifers* (A. B. Klimchouk, D. C. Ford, A. N. Palmer & W. Dreybrodt, eds.), pp. 91–99. National Speleological Society, Huntsville, AL, USA.

Kovács, A., Perrochet, P., Király, L. & Jeannin, P.-Y. 2005 A quantitative method for the characterisation of karst aquifers based on spring hydrograph analysis. *J. Hydrol.* **303** (1–4), 152–164.

Lamb, R. & Beven, K. J. 1997 Using interactive recession curve analysis to specify a general catchment storage model. *Hydrol. Earth Syst. Sci.* **1**, 101–113.

Li, R. L., Wang, S. J. & Zhang, D. F. 2002 The role of man-made factors in eco-environmental deterioration in guizhou karst areas. *Bulletin of Mineralogy Petrology and Geochemistry* **21** (1), 43–47.

Li, X. Z. 2001 Evolution of karst geomorphology of upper cenozoic and its influential factors in Guizhou plateau. *Guizhou Geology* **18** (1), 29–36.

Milanovic, P. T. 1981 *Karst Hydrogeology*. Water Resour. Publ., Littleton, Colo., 434 pp.

Padilla, A., Pulido-Bosch, A. & Mangin, A. 1994 Relative importance of baseflow and quickflow from hydrographs of karst spring. *Ground Water* **32** (2), 267–277.

Rorabaugh, M. I. 1964 Estimating changes in bank storage as ground-water contribution to streamflow. *Int. Assoc. Sci. Hydrol. Publ.* **63**, 432–441.

Sauter, M. 1992. Quantification and Forecasting of Regional Groundwater Flow and Transport in a Karst Aquifer (Gallusquelle, Malm, SW Germany). Tübingen Geowissenschaftliche Arbeiten, Reihe C, 13, Tübingen.

Shevenell, L. 1996 Analysis of well hydrographs in a karst aquifer: estimates of specific yields and continuum transmissivities. *J. Hydrol.* **174** (3–4), 331–355.

Singhal, B. B. S. & Gupta, R. P. 1999 *Applied Hydrogeology of Fractured Rocks*. Kluwer Academic Publishers, Dordrecht, The Netherlands.

Teutsch, G. 1992 Groundwater modeling in karst terranes: scale effects, data acquisition and field validation. *Ground Water Manage* **10**, 17–35.

Trček, B. 2007 How can the epikarst zone influence the karst aquifer hydraulic behaviour? *Environ Geol.* **51**, 761–765.

Wang, M. 1999 Discussion on the development of karst stone underground water of karst mountainous region, Guizhou. *Guizhou Geology* **16** (3), 259–265.

Williams, P. W. 1983 The role of the subcutaneous zone in karst hydrology. *J Hydrol.* **61**, 45–67.

Williams, P. W. 2008 The role of the epikarst in karst and cave hydrogeology: a review. *Int. J. Speleology* **37** (1), 1–10.

Yang, M. D. 1982 The geomorphologic regularities of karst water occurrences in the Guizhou plateau. *Carsologica Sinica* **2**, 81–91.

Yang, T., Chen, X., Xu, C. Y. & Zhang, Z. C. 2009 Spatio-temporal changes of hydrological processes and underlying driving forces in Guizhou region, Southwest China. *Stoch. Env. Res. Risk. A.* **23** (8), 1071–1087.

Yuan, D. X. & Cai, G. M. 1988 *The Science of Karst Environment*. Chongqing Press (in Chinese), Chongqing, China.

Zeng, Z. 1994 Suggestion on poverty-deviation in the karst mountain areas in south China. In: *Human Activity and Karst Environment* (Y. H. Xie & M. D. Yang, eds.) Beijing Science and Technology Press, Beijing, pp. 15–19 (in Chinese).

First received 8 October 2009; accepted in revised form 22 November 2010. Available online December 2011